Distribution Agreement

In presenting this thesis or dissertation as a partial fulfillment of the requirements for an advanced degree from Emory University, I hereby grant to Emory University and its agents the non-exclusive license to archive, make accessible, and display my thesis or dissertation in whole or in part in all forms of media, now or hereafter known, including display on the world wide web. I understand that I may select some access restrictions as part of the online submission of this thesis or dissertation. I retain all ownership rights to the copyright of the thesis or dissertation. I also retain the right to use in future works (such as articles or books) all or part of this thesis or dissertation.

Caitlin McConaghy 04/17/2023

Association between the El Niño Southern Oscillation (ENSO) and levels of legacy persistent organic pollutants measured in Alaskan seabird eggs from 1999 to 2010

By

Caitlin McConaghy
Master of Public Health

Global Environmental Health

Amina Salamova, PhD
Committee Chair

Matthew Gribble, PhD
Committee Member

Vrinda Kalia, PhD
Committee Member

Association between the El Niño Southern Oscillation (ENSO) and levels of legacy persistent organic pollutants measured in Alaskan seabird eggs from 1999 to 2010

By

Caitlin McConaghy

B.S., The Ohio State University, 2020

Thesis Committee Chair: Amina Salamova, PhD

An abstract of
a thesis submitted to the Faculty of the
Rollins School of Public Health of Emory University
in partial fulfillment of the requirements for the degree of
Master of Public Health
in Global Environmental Health
2023

Abstract

Association between the El Niño Southern Oscillation (ENSO) and levels of legacy persistent organic pollutants measured in Alaskan seabird eggs from 1999 to 2010

By Caitlin McConaghy

Legacy persistent organic pollutants (POPs) are predicted to remobilize in the environment due to warming global temperatures, underscoring the importance of examining the relationship between large-scale climate oscillations and the ecotoxicology of POPs. In this paper, we model the association between the El Niño Southern Oscillation (ENSO), a measure of Pacific sea surface temperature (SST) variability, and levels of polychlorinated biphenyls (PCBs), organochlorine pesticides (OCPs), and polybrominated diphenyl ethers (PBDEs) measured in sympatric seabird eggs collected from the Gulf of Alaska and the Bering Sea between 1999 and 2010. The warm and cool phases of the ENSO predicted contaminant loads in both common murre and thick-billed murre eggs. We found an inverse pattern of bioaccumulation between the two species, likely due to differences in foraging behavior. Relative contribution of individual congeners to total PCBs in the sample predicted the magnitude of association between ENSO and PCB levels measured the eggs of both species. The results of this study suggest that the ENSO may be an important determinant of POP ecotoxicology in Alaska and should be considered in pollutant monitoring and human exposure assessments.

Association between the El Niño Southern Oscillation (ENSO) and levels of legacy persistent organic pollutants measured in Alaskan seabird eggs from 1999 to 2010

By

Caitlin McConaghy

B.S., The Ohio State University, 2020

Thesis Committee Chair: Amina Salamova, PhD

A thesis submitted to the Faculty of the
Rollins School of Public Health of Emory University
in partial fulfillment of the requirements for the degree of
Master of Public Health
in Global Environmental Health
2023

Contents

Introduction

Persistent organic pollutants (POPs) are chemicals that persist in the environment, accumulating in both abiotic and biotic reservoirs, and are found ubiquitously in various environmental matrices. These compounds are subject to long-range atmospheric transport toward higher latitudes, a process known as global fractionation (Burkow and Kallenborn 2000, Vander Pol, Becker et al. 2004), where they deposit and enter the marine food web (Eulaers, Jaspers et al. 2013). Consequently, inhabitants of the circumpolar north are at increased risk of dietary exposure to POPs (Armitage, Quinn et al. 2011). This is especially true for indigenous peoples, like the Inuit, for whom the consumption of fish, marine mammals, and seabird eggs is nutritionally and culturally important (Czub, Wania et al. 2008).

Though global levels of many legacy POPs, such as organochlorine pesticides (OCPs) and industrial chemicals, have declined due to regulatory action of primary emissions, global climate change may alter planetary processes in ways that cause them to remobilize within the environment (Armitage, Quinn et al. 2011, Balbus, Boxall et al. 2013). Higher ambient temperatures are predicted to cause the release of previously sequestered pollutants via sea and glacial ice melt and thawing permafrost, thereby increasing secondary emissions. Rising temperatures may also enhance the partitioning of contaminants from the water column into the atmosphere (Noyes, McElwee et al. 2009). This trend is evident in the European Arctic, where atmospheric polychlorinated biphenyl (PCB) levels have demonstrated a slower rate of decline since 2000, likely due to remobilization (Borga, McKinney et al. 2022).

Exposure pathways among Arctic biota are also subject to climate processes. Sea surface temperature (SST) affects ice cover which, in turn, influences both trophic dynamics and primary production of algae (Gaston, Gilchrist et al. 2009, Braune, Gaston et al. 2015). Bioavailability of contaminants up the food chain is likely to increase in response to organic matter growth (Hooper, Ankley et al. 2013). Higher ambient temperatures have also been associated with accelerated uptake and elimination of contaminants and altered lipid dynamics in wildlife.

Occurring in tandem with global climate change are natural climate variation patterns like the Arctic Oscillation (AO), North Atlantic Oscillation (NAO), Pacific Decadal Oscillation (PDO). A previous study explored the association between the AO and NAO and environmental contaminant trends in the Norwegian and Greenlandic Arctic, finding that concentrations of POPs were higher in glaucous gulls (*Larus hyperboreus*) and ringed seals (*Pusa hispida*) following periods of increased air transport toward the Arctic (Borga, McKinney et al. 2022). In the Canadian Arctic, time-lagged concentrations of organochlorines measured in thick-billed murre (*Uria lomvia*) and northern fulmar (*Fulmarus glacialis*) eggs were also found to be positively associated with the NAO. Another study found an association between the PDO and levels of organochlorine compounds measured in Alaskan thick-billed murre eggs (Kalia, Schuur et al. 2021).

The El Niño Southern Oscillation (ENSO) is another large-scale climate cycle that describes interannual SST variability originating in the equatorial Pacific Ocean. The ENSO is defined numerically, with positive indices indicating the warm (El Niño) phase, characterized by above-average SST and weak easterly winds; while negative indices

constitute the cool (La Niña) phase, characterized by below-average SST and strong easterly winds. Altered atmospheric convection and precipitation patterns are felt primarily in the tropics, with secondary impacts extending up through the North Pacific (Mantua 2017). To our knowledge, there is a gap in the literature examining the relationship between the ENSO and environmental contaminant levels in the circumpolar north. In this paper, we seek to fill this gap by modeling the association between the ENSO and levels of legacy POPs measured in Alaskan seabird eggs.

Materials

Contaminant Data

We examined levels of legacy POPs measured in common murre (*Uria aalge*) and thick-billed murres eggs, two sympatric seabird species with different feeding ecology. Both species occupy upper trophic positions within circumpolar marine food webs, though thick-billed murres demonstrate greater trophic flexibility (Kalia, Schuur et al. 2021). Because circumpolar marine food webs are characterized by high lipid concentrations and many trophic levels, lipophilic contaminants accumulate to a higher degree along the food chain (Fisk, de Wit et al. 2005, Czub, Wania et al. 2008). Murres lay only one egg per year during which contaminants are transferred, along with fatty tissue, from mother to egg (Braune, Gaston et al. 2019). Contaminant levels measured in murre eggs therefore mirror contaminant levels in the female bird during egg formation. Thus, murre eggs are effective sentinels for health of the environment and can indicate toxicant exposure risk to humans (Bustnes, Bardsen et al. 2022).

Pollutant data were obtained through an access policy from the Seabird Tissue Archival Monitoring Project (STAMP), a consortium of government agencies, non-governmental organizations, and Alaska Native groups, which measures pollutant levels in seabird eggs to monitor the health of Alaska's marine environment. Standard STAMP protocols for collecting and processing seabird eggs, banking the specimens, and performing sample extraction and analysis have been described in detail in previous papers (Vander Pol, Christopher et al. 2003, Vander Pol, Becker et al. 2009, Vander Pol, Becker et al. 2012, Mahynski, Ragland et al. 2021).

For PCBs, OCPs, and polybrominated diphenyl ethers (PBDEs), samples were extracted by pressurized fluid extraction (PFE), using sodium sulfate or diatomaceous earth, and further cleaned with PFE and size exclusion chromatography (SEC) followed by semi-prep aminopropyl silane fractionation or solid phase extraction (SPE). Samples were analyzed using gas chromatography (GC) with electron capture detection or GC-mass spectrometry. For quality assurance, procedural blanks, NIST ®SRM 1946 - Lake Superior fish tissue (for eggs collected in 1999 to 2001) and in-house murre egg control material (for eggs collected after 2001) were included in batch analyses. POPs analyzed between 1999 and 2001 were assigned a detectable limit of 0.100 ng/g wet mass. For compounds analyzed after 2001, limits of Detection (LOD) were determined by dividing the lowest observable calibration solutions by the sample masses, and limits of quantification (LOQ) were determined by dividing the average blank values plus three times the standard deviations by the sample masses. Prior to analysis, pollutant levels at LOD/LOQ were replaced with $\frac{(LOD/LOQ)}{\sqrt{2}}$.

STAMP data included information on fifty-seven PCB congeners, twelve OCPs, and three PBDEs measured in 213 common murre and thick-billed murre eggs collected from nesting colonies within the Bering Sea, Gulf of Alaska, and Norton Sound between 1999 and 2010. Because only 15 eggs were collected from Norton Sound, all of which were common murre eggs, observations from Norton Sound were excluded from the analysis, reducing the study population's sample size to 198 eggs: 97 common murre eggs and 101 thick-billed murre eggs. Eggs from each species were collected from the Bering Sea and Gulf of Alaska at least one time in every three years. Neither common murre eggs nor thick-billed murre eggs were collected in 2007. Sample information is included in **Table 1**.

Climate Data

To study the association between the ENSO and levels of pollutants measured in Alaskan seabird eggs, we used the Oceanic Niño Index (ONI), one of the most common indices used to determine El Niño and La Niña events. The ONI, which uses a 3-month running average, measures regional SST in the tropical Pacific Ocean from the International Date Line to the coast of South America (5N-5S, 170W-120W) (NCAR n.d.). A positive ONI is an indicator of the El Niño phase, while a negative ONI indicates presence of the La Niña, or cool, phase. To be classified as a full El Niño or La Niña event by the National Oceanic and Atmospheric Association (NOAA), SST anomalies in the equatorial Pacific must exceed +0.5°C or -0.5°C, respectively, for at least five consecutive months (NCAR n.d.). Average annual ONI indices for each year from 1999 to 2010 were retrieved from the NOAA/Physical Sciences Laboratory at https://psl.noaa.gov/enso/data.html.

Like the ENSO, the PDO is a natural and recurring global cycle of ocean-atmosphere climate variation with both a warm and a cool phase, though it occurs on a longer timescale. The PDO index is a measure of monthly SST variability in the North Pacific Ocean, poleward of 20N latitude (Mantua 2017). A previous study by Kalia and colleagues, using STAMP data, found an association between POP levels in thick-billed murre eggs and PDO index averaged each year during egg-laying season (February to May) (Kalia, Schuur et al. 2021). Therefore, we included PDO as a covariate in our model. Seasonally averaged PDO indices for each year from 1999 to 2010 were retrieved from the University of Washington, in partnership with the NOAA, at http://research.jisao.washington.edu/pdo/.

Methods

Data Management

Data management was performed in STATA 17.0 S/E (StataCorp, College Station, Texas). Pollutant levels were lipid-adjusted by dividing contaminant level by lipid content and multiplying by one hundred, then natural log-transformed. Included in the analysis for common murres were fifty-two PCB congeners (some of which co-eluted in the analytical method): PCB 28 + 31, 49, 52, 56, 66, 70, 74, 87, 92, 99, 101, 105, 106, 114, 118, 119, 128, 130, 137, 138, 146, 153 + 132, 154, 157, 158, 163, 165, 166, 167, 170, 172, 174, 175, 177, 178, 180 + 193, 183, 187, 188, 189, 191, 194, 195, 196, 197, 199, 201, 202, 205, 206, 207, and 208; nine OCPs: alpha–hexachlorocyclohexane (α-HCH), hexachlorobenzene (HCB), perchloropentacyclodecane (mirex), 2,4′-dichlorodiphenyldichloroethylene (2,4′-DDE), 4,4′-dichlorodiphenyldichloroethylene

(4,4′-DDE), *cis*-chlordane, *cis*-nonachlor, epoxyheptachlor (heptachlor epoxide), and octachlor epoxide (oxychloradane); and three PBDEs: BDE 47, 99, and 100.

The analysis for thick-billed murres included the same compounds except for PCBs 74, 119, 137, 167, and 174; mirex; and *cis*-chlordane. Additional compounds included in the analysis for thick-billed murres were PCBs 63, 149, 156 + 202 + 171, and 209; oxychlordane; and dieldrin. In total, fifty-one PCB congeners/coelutions, eight OCPs, and three PBDEs measured in thick-billed murre eggs were analyzed.

Log-linear Spline Regression

Piecewise linear spline regression was used to model the association between annual average ONI index and log-transformed, lipid-adjusted contaminant levels measured in the eggs of common murres and thick-billed murres collected from colonies in the Gulf of Alaska and the Bering Sea between 1999 and 2010. The ENSO cycle is in the El Niño (warm) phase when ONI indices are positive and in the La Niña (cool) phase when ONI indices are negative. Therefore, a spline knot was created at ONI = 0 to allow for possible differences in the association between contaminant level and ONI index between the El Niño and La Niña phases. Seasonally averaged (February to May) PDO index was included as a covariate in the model. Like the ENSO, the PDO is in its warm phase when PDO index is positive and in its cool phase when PDO index is negative. Therefore, a spline knot was created at PDO index = 0 to allow for possible heterogeneity between phases. The model was also adjusted for year and location (Gulf of Alaska or Bering Sea) of egg collection.

Non-parametric bootstrap, assuming independent observations, with replacement (seed: 13297, replicates: 1000) was used to estimate 95% normal and bias-

corrected and accelerated (BCa) confidence intervals (CIs) for each contaminant's regression coefficient. Normal and BCa CIs are shown in **Table 2** for common murres and in **Table 3** for thick-billed murres.

Model Specification

For contaminant (PCB, OCP, or PBDE) *c* and for bird *j*, log-transformed and lipid-adjusted contaminant level *b*, intercept α, ONI index *n*, indicator variables $I_n<0$ or $I_n>0$ for when ONI index is negative or positive, PDO index *p*, indicator variables $I_p<0$ or $I_p>0$ for when PDO index is negative or positive, year *t,* and waterbodies (Gulf of Alaska or Bering Sea) W_1 and W_2:

$$\ln b_{j,c} = \alpha + (I_{n<0})(n_j)\beta_1 + (I_{n>0})(n_j)\beta_2 + (I_{p<0})(p_j)\beta_3 + (I_{p>0})(p_j)\beta_4 + (t_j)\beta_5 + (t^2_j)\beta_6 + (W_{1,j})\beta_7 + (W_{2,j})\beta_8 + \varepsilon_{j,c}$$

$$\varepsilon_{j,c} \sim N(0,\tau^2_c)$$

where τ^2_c is the residual variance.

Meta-Regression

To examine the heterogeneity in association between the ONI and PCB levels measured in common and thick-billed murre eggs, we input the regression coefficients from the bootstrapped piecewise log-linear spline regression models for each congener into a random effects restricted maximum likelihood (REML) meta-regression. We first conditioned on the number of chlorine groups on each congener. Lighter congeners are more volatile and degrade more quickly in the atmosphere (Beyer, Mackay et al. 2000, Hung, Lee et al. 2005). Heavier congeners tend to persist longer in the environment and

sequester in the deep sea via particle deposition, rather than undergoing atmospheric degradation.

We were also interested in examining whether the relative contribution of each congener within our sample influenced the observed ENSO-related changes in PCB levels measured in common and thick-billed murres eggs. We therefore performed a second meta-regression of the coefficients, conditioning on relative contribution. To calculate relative contribution, we did the following: for each observation, the level of each individual congener measured in that egg was divided by the sum of all congeners (total PCB concentration) in that egg. The contributions of individual congeners to the total were then averaged across all observations to get the percent contribution of each congener within the sample. Relative contribution for PCB congeners are shown in **Table 4** along with measurement frequency, calculated by dividing the number of eggs in which each congener was measured by the total number of eggs in the sample.

Sensitivity Analysis

We excluded PCB congeners that contributed less than 3% of the total PCBs in the sample. Eleven congeners remained, representing the most abundant PCBs in the sample. Coefficients from the piecewise log-linear spline regressions for these congeners were used in a random effects REML meta-analysis summary.

Results

Thick-billed Murres

When the ENSO was in its El Niño phase, PCB congener levels measured in thick-billed murre eggs were positively associated with the ONI. When the ENSO was in its La

Niña phase, PCB congener levels measured in thick-billed murre eggs were negatively associated with the ONI. This pattern was generally consistent across all congeners, except for PCBs 63, 149, 157, 194, 202, 206, and 209, all of which are minor congeners each contributing less than 3% of total PCBs in the sample. A random effects REML meta-regression found the pooled estimate across all PCB congeners to be 0.887 (95% confidence interval: 0.674, 1.099) during the El Niño phase and -0.892 (95% confidence interval: -1.400, -0.384) during the La Niña phase. The percent change in PCB level, averaged across all congeners, associated with one unit increase in ONI was estimated to be $100 \times (e^{0.887} - 1) \approx 143\%$ during the El Niño phase and $100 \times (e^{-0.892} - 1) \approx -59.0\%$ during the La Niña phase.

Sensitivity analysis excluding congeners that constituted less than 3% of the total PCBs did not change the association between the ONI and PCB levels measured in thick-billed murre eggs. A random effects REML meta-analysis summary found the pooled estimate across the eleven congeners with the highest relative contribution to be 1.116 (95% confidence interval: 0.783, 1.448) during the El Niño phase and -1.248 (95% confidence interval: -1.511, -0.984) during the La Niña phase, in thick-billed murres.

PBDE levels measured in thick-billed murre eggs were also positively associated with the ONI during the El Niño phase, with a pooled estimate of 1.890 (95% confidence interval: 0.647, 3.133), but demonstrated no significant association with the ONI during the La Niña phase. The percent change during the El Niño phase, averaged across all PBDEs, was estimated to be $100 \times (e^{1.890} - 1) \approx 562\%$ for each single unit increase in ONI.

There was no clear pattern of association between ONI and OCP levels measured in thick-billed murre eggs during either phase of the ENSO. Associations between the ONI and contaminant levels in thick-billed murres are shown in **Figure 1**.

Common Murres

When the ENSO was in its El Niño phase, PCB congener levels measured in common murre eggs were negatively associated with the ONI. A random effects REML meta-regression found the pooled estimate across all congeners to be -0.722 (95% confidence interval: -0.894, -0.549) during the El Niño phase. During the La Niña phase, PCB levels measured in common murre eggs were positively associated with the ONI, with a pooled estimate of 0.333 (95% confidence interval: 0.185, 0.481). The average PCB level across all congeners was expected to change by $100 \times (e^{-0.722} - 1) \approx -51.4\%$ during the El Niño phase and $100 \times (e^{0.333} - 1) \approx 39.5\%$ during the La Niña phase, for every one unit increase in the ONI.

During the La Niña phase, sensitivity analysis excluding congeners that constituted less than 3% of the total PCBs changed the association between the ONI and PCB levels measured in common murre eggs from positive to negative, while this association remained consistent during the El Niño phase. A random effects REML meta-analysis summary found the pooled estimate across the eleven congeners with the highest relative contribution to be -0.353 (95% confidence interval: -0.553, -0.154) during the El Niño phase and -0.148 (95% confidence interval: -0.266, -0.029) during the La Niña phase, in common murres.

PBDE levels in common murre eggs were negatively associated with the ONI during the El Niño phase (pooled estimate: -1.572; 95% confidence interval: -2.357, -

0.787), but were not associated with the ONI during the La Niña phase. The estimated percent change, averaged across all PBDEs, was $100 \times (e^{-1.572} - 1) \approx -79.2\%$ for each single unit increase in ONI.

When the ENSO was in its El Niño phase, there was a negative association between the ONI and OCP levels measured in common murre eggs. This association turned positive during the La Niña phase. The pooled estimates across all pesticides from the random effects REML meta-analysis were -0.271 (95% confidence interval: -0.436, -0.105) and 0.259 (95% confidence interval: 0.004, 0.515) during the El Niño and La Niña phases, respectively. The percent change in contaminant level, averaged across all OCPs, associated with one unit increase in ONI was estimated to be $100 \times (e^{-0.271} - 1) \approx -23.7\%$ during the El Niño phase and $100 \times (e^{0.259} - 1) \approx 129\%$ during the La Niña phase. Associations between the ONI and contaminant levels in common murres are shown in **Figure 2**.

Meta-Regression

In thick-billed murres, the relative contribution of each congener to the sum of congeners did not significantly influence the PDO-, year-, and waterbody-adjusted association between ENSO index and PCB congener levels during the La Nina phase ($p = 0.162$). During the El Niño phase, this association became increasingly and significantly positive with increasing relative abundance ($p = 0.038$) [**Figure 3**].

In common murres, the association between ONI and PCB congener levels, adjusted for PDO index, year, and waterbody, was more positive among the least-abundant congeners and less positive among the most-abundant congeners during the La Niña phase ($p = 0.013$). During the El Niño phase, this association, though not

statistically significant, was more negative among the least-abundant congeners and became less negative among the most-abundant congeners ($p = 0.097$) [**Figure 4**].

For both common murres and thick-billed murres, the chlorine content of each congener did not influence the PDO-, year-, and waterbody-adjusted association between the ONI and PCB levels in either ENSO phase.

Discussion

We found an association between the ONI and levels of legacy POPs measured in the eggs of two sympatric Alaskan seabird species, indicating that ENSO-related SST variability may influence the fate of chemicals within the Alaskan environment. The observed differences in bioaccumulation patterns between common murres and thick-billed murres, which have different trophic flexibility, suggest that feeding ecology moderates the relationship between the ENSO and chemical uptake within the marine food webs of this region.

In thick-billed murres, PCB and PBDE levels generally increased with the ONI during the El Niño phase and decreased with the ONI during the La Niña phase. OCPs in thick-billed murres did not demonstrate a clear pattern of association with the ONI, perhaps due to different rates of environmental decline among compounds. For instance, time-series analyses suggest that levels of α-HCH, and DDE in Arctic biota are declining rapidly, while HCB and chlordanes are declining more slowly or displaying mixed trends (Riget, Bignert et al. 2010, Riget, Bignert et al. 2019). In common murres, POPs generally decreased with the ONI during the El Niño phase and increased with the ONI during the La Niña phase.

The inverse pattern of bioaccumulation between the two species is likely due to species-specific differences in feeding ecology. Common murres forage in the mesopelagic zone, whereas thick-billed murres dive deeper, also consuming benthic organisms (Gaston and Hipfner 2000, Ainley, Nettleship et al. 2002). Climate-related shifts in trophic dynamics can alter the flow of carbon between pelagic and benthic food webs, thereby altering biomagnification pathways of organochlorines (Macdonald, Harner et al. 2005).

In our study, a random effects REML meta-regression did not find the number of chlorines on each PCB congener to be a strong predictor of the association between the ONI and PCB level in either species. This was unexpected, as we assumed that congeners with a higher chlorine content would be less sensitive to SST anomalies, as was found to be the case in a previous study (Kalia, Schuur et al. 2021). This could be because our sample did not have many light congeners (with only three or four chlorine groups) which are more volatile and less bioaccumulative.

The PCB congeners with the highest relative contributions in our sample were PCB 118 (10.10%), PCB 138 (8.60%), and PCB 153+132 (19.37%), all of which are penta- or hexa-chlorinated congeners, which were industrially produced more frequently than other congeners and have a higher bioaccumulation potential (Borga, Gabrielsen et al. 2001, Braune, Gaston et al. 2019). All four have documented adverse consequences to human and animal health (Faroon and Ruiz 2016).

Relative contribution of each congener to total PCBs may partially explain the heterogeneity in association between PCB level and ONI. In thick-billed murre eggs, this association became more strongly positive with increasing relative contribution during

the El Niño phase, and more strongly negative with increasing relative contribution during the La Niña phase. In contrast, the association between PCB levels in common murres and the ONI, during both ENSO phases, appeared to weaken with increasing relative contribution.

Limitations

We bootstrapped individual observations (seabird eggs) and therefore could not account for clustering by nesting colonies. Our analysis also does not consider possible time-lag between ENSO and subsequent effects on POPs. Moreover, the PDO is believed to modulate the ENSO, either amplifying or diminishing its effects depending on whether the warm and cool phases of both cycles are in sync, suggesting effect modification. However, the phases of the ENSO and PDO were highly collinear during our study period, so we were unable to include an interaction term in our model. Further, our model does not consider overwintering, which may be a source of contaminant exposure among migratory birds (Noyes, McElwee et al. 2009).

Conclusions

Under a warmer climate, POPs are predicted to mobilize from surface media into the atmosphere, accelerating global fractionation. At the same time, higher temperatures may accelerate the atmospheric degradation of these compounds (Balbus, Boxall et al. 2013, Hansen, Christensen et al. 2015). The predicted net change in transport of POPs to the circumpolar north will depend on their physiochemical properties. Occurring in tandem with global climate change are large-scale climate oscillations. It is important to characterize the influence of these natural patterns of

climate variability on contaminants within the circumpolar north, especially given this region's vulnerability to climate impacts.

The results of this study suggest that the ENSO is an important determinant of the fate of legacy POPs within Alaskan marine food webs. Inhabitants of this region are exposed to these chemicals via consumption of upper trophic level species. Consequently, human exposure to POPs may also be influenced by the ENSO. Many halogenated POPs are considered carcinogens and endocrine disruptors and have been associated with neurologic and reproductive dysfunction (Balbus, Boxall et al. 2013). Ecotoxicological monitoring efforts in Alaska should therefore consider the ENSO and its implications for assessing human exposure.

References

Ainley, D. G., D. N. Nettleship, H. R. Carter and A. E. Storey. (2002). "Common Murre (*Uria aalge*)." The Birds of North America version 2.0.

Armitage, J. M., C. L. Quinn and F. Wania (2011). "Global climate change and contaminants-an overview of opportunities and priorities for modelling the potential implications for long-term human exposure to organic compounds in the Arctic." Journal of Environmental Monitoring **13**(6): 1532-1546.

Balbus, J. M., A. B. A. Boxall, R. A. Fenske, T. E. McKone and L. Zeise (2013). "Implications of global climate change for the assessment and management of human health risks of chemicals in the natural environment." Environmental Toxicology and Chemistry **32**(1): 62-78.

Beyer, A., D. Mackay, M. Matthies, F. Wania and E. Webster (2000). "Assessing long-range transport potential of persistent organic pollutants." Environmental Science & Technology **34**(4): 699-703.

Borga, K., G. W. Gabrielsen and J. U. Skaare (2001). "Biomagnification of organochlorines along a Barents Sea food chain." Environmental Pollution **113**(2): 187-198.

Borga, K., M. A. McKinney, H. Routti, K. J. Fernie, J. Giebichenstein, I. Hallanger and D. C. G. Muir (2022). "The influence of global climate change on accumulation and toxicity of persistent organic pollutants and chemicals of emerging concern in Arctic food webs." Environmental Science-Processes & Impacts **24**(10): 1544-1576.

Braune, B. M., A. J. Gaston, K. A. Hobson, H. G. Gilchrist and M. L. Mallory (2015). "Changes in trophic position affect rates of contaminant decline at two seabird colonies in the Canadian Arctic." Ecotoxicology and Environmental Safety **115**: 7-13.

Braune, B. M., A. J. Gaston and M. L. Mallory (2019). "Temporal trends of legacy organochlorines in eggs of Canadian Arctic seabirds monitored over four decades." Science of the Total Environment **646**: 551-563.

Burkow, I. C. and R. Kallenborn (2000). "Sources and transport of persistent pollutants to the Arctic." Toxicology Letters **112**: 87-92.

Bustnes, J. O., B. J. Bardsen, D. Herzke, G. Bangjord, E. Bollinger, S. Bourgeon, R. Schulz, C. Fritsch and I. Eulaers (2022). "The impact of climate sensitive factors on the exposure to organohalogenated contaminants in an aquatic bird exploiting both marine and freshwater habitats." Science of the Total Environment **850**.

Czub, G., F. Wania and M. S. McLachlan (2008). "Combining long-range transport and bioaccumulation considerations to identify potential arctic contaminants." Environmental Science & Technology **42**(10): 3704-3709.

Eulaers, I., V. L. B. Jaspers, J. O. Bustnes, A. Covaci, T. V. Johnsen, D. J. Halley, T. Moum, R. A. Ims, S. A. Hanssen, K. E. Erikstad, D. Herzke, C. Sonne, M. Ballesteros, R. Pinxten and M. Eens (2013). "Ecological and spatial factors drive intra- and interspecific variation in exposure of subarctic predatory bird nestlings to persistent organic pollutants." Environment International **57-58**: 25-33.

Faroon, O. and P. Ruiz (2016). "Polychlorinated biphenyls: New evidence from the last decade." Toxicology and Industrial Health **32**(11): 1825-1847.

Fisk, A. T., C. A. de Wit, M. Wayland, Z. Z. Kuzyk, N. Burgess, R. Robert, B. Braune, R. Norstrom, S. P. Blum, C. Sandau, E. Lie, H. J. S. Larsen, J. U. Skaare and D. C. G. Muir (2005). "An assessment of the toxicological significance of anthropogenic contaminants in Canadian arctic wildlife." Science of the Total Environment **351**: 57-93.

Gaston, A. J. and J. M. Hipfner. (2000). "Thick-billed Murre (*Uria lomvia*)." The Birds of North America version 2.0.

Gaston, A. T., H. G. Gilchrist, M. L. Mallory and P. A. Smith (2009). "CHANGES IN SEASONAL EVENTS, PEAK FOOD AVAILABILITY, AND CONSEQUENT BREEDING ADJUSTMENT IN A MARINE BIRD: A CASE OF PROGRESSIVE MISMATCHING." Condor **111**(1): 111-119.

Hansen, K. M., J. H. Christensen, C. Geels, J. D. Silver and J. Brandt (2015). "Modelling the impact of climate change on the atmospheric transport and the fate of persistent organic pollutants in the Arctic." Atmos. Chem. Phys. **15**(11): 6549-6559.

Hooper, M. J., G. T. Ankley, D. A. Cristol, L. A. Maryoung, P. D. Noyes and K. E. Pinkerton (2013). "Interactions between chemical and climate stressors: A role for mechanistic toxicology in assessing climate change risks." Environmental Toxicology and Chemistry **32**(1): 32-48.

Hung, H., S. C. Lee, F. Wania, P. Blanchard and K. Brice (2005). "Measuring and simulating atmospheric concentration trends of polychlorinated biphenyls in the Northern Hemisphere." Atmospheric Environment **39**(35): 6502-6512.

Kalia, V., S. S. Schuur, K. A. Hobson, H. H. Chang, L. A. Waller, S. R. Hare and M. O. Gribble (2021). "Relationship between the Pacific Decadal Oscillation (PDO) and persistent organic pollutants in sympatric Alaskan seabird (Uria aalge and U. lomvia) eggs between 1999 and 2010." Chemosphere **262**.

Macdonald, R. W., T. Harner and J. Fyfe (2005). "Recent climate change in the Arctic and its impact on contaminant pathways and interpretation of temporal trend data." Science of The Total Environment **342**(1): 5-86.

Mahynski, N. A., J. M. Ragland, S. S. Schuur, R. Pugh and V. K. Shen (2021). "Seabird Tissue Archival and Monitoring Project (STAMP) Data from 1999-2010." Journal of Research of the National Institute of Standards and Technology **126**: 1-7.

Mantua, N. (2017). "The Pacific Decadal Oscillation (PDO)." Retrieved June 28, 2022, from http://research.jisao.washington.edu/pdo/.

NCAR. (n.d.). "Niño SST Indices (Niño 1+2, 3, 3.4, 4; ONI and TNI)." Retrieved June 28, 2022, from https://climatedataguide.ucar.edu/climate-data/nino-sst-indices-nino-12-3-34-4-oni-and-tni.

Noyes, P. D., M. K. McElwee, H. D. Miller, B. W. Clark, L. A. Van Tiem, K. C. Walcott, K. N. Erwin and E. D. Levin (2009). "The toxicology of climate change: Environmental contaminants in a warming world." Environment International **35**(6): 971-986.

Riget, F., A. Bignert, B. Braune, M. Dam, R. Dietz, M. Evans, N. Green, H. Gunnlaugsdottir, K. S. Hoydal, J. Kucklick, R. Letcher, D. Muir, S. Schuur, C. Sonne, G. Stern, G. Tomy, K. Vorkamp and S. Wilson (2019). "Temporal trends of

persistent organic pollutants in Arctic marine and freshwater biota." Science of the Total Environment **649**: 99-110.

Riget, F., A. Bignert, B. Braune, J. Stow and S. Wilson (2010). "Temporal trends of legacy POPs in Arctic biota, an update." Science of the Total Environment **408**(15): 2874-2884.

Vander Pol, S. S., P. R. Becker, S. Berail, R. D. Day, O. F. Donard, K. A. Hobson, A. J. Moors, R. S. Pugh, L. B. Rust and D. G. Roseneau (2012). SEABIRD TISSUE ARCHIVAL AND MONITORING PROJECT: Egg Collections and Analytical Results for 2006-2009, NIST Interagency/Internal Report (NISTIR). Gaithersburg, MD [online], National Institute of Standards and Technology.

Vander Pol, S. S., P. R. Becker, R. D. Day, M. B. Ellisor, A. Guichard, A. J. Moors, D. Point, R. S. Pugh and D. G. Roseneau (2009). SEABIRD TISSUE ARCHIVAL AND MONITORING PROJECT: Egg Collections and Analytical Results for 2002-2005, NIST Interagency/Internal Report (NISTIR). Gaithersburg, MD [online], National Institute of Standards and Technology.

Vander Pol, S. S., P. R. Becker, J. R. Kucklick, R. S. Pugh, D. G. Roseneau and K. S. Simac (2004). "Persistent Organic Pollutants in Alaskan Murre (Uria spp.) Eggs: Geographical, Species, and Temporal Comparisons." Environmental Science & Technology **38**(5): 1305-1312.

Vander Pol, S. S., S. J. Christopher, D. G. Roseneau, P. R. Becker, R. D. Day, J. R. Kucklick, R. S. Pugh, K. S. Simac and G. W. York (2003). SEABIRD TISSUE ARCHIVAL AND MONITORING PROJECT: Egg Collections and Analytical

Results for 1999-2002, NIST Interagency/Internal Report (NISTIR).

Gaithersburg, MD [online], National Institute of Standards and Technology.

Tables and Figures

Table 1. Number of eggs sampled across years (1999-2010), stratified by bird species (common murre and thick-billed murre) and waterbody from which each egg was collected (Bering Sea and Gulf of Alaska). There were no eggs collected in 2007.

	YEAR											
	1999	2000	2001	2002	2003	2004	2005	2006	2008	2009	2010	Total
Common Murre (*Uria aalge*)												
Bering Sea	11	0	0	3	0	5	0	10	5	5	5	44
Gulf of Alaska	10	0	10	0	10	8	0	5	5	0	5	53
Thick-billed Murre (*Uria lomvia*)												
Bering Sea	0	7	0	13	5	5	5	10	10	0	10	65
Gulf of Alaska	0	0	10	6	0	5	0	5	5	0	5	36

Table 2. Comparison of bootstrapped normal (N) and bias-corrected and accelerated (BCa) 95% confidence intervals (CIs) of the coefficients from the piecewise log-linear spline regression models for each contaminant measured in common murre eggs.

	La Niña Phase						El Niño Phase					
Contaminant	Regression Coefficient	P-value	N CI Lower	N CI Upper	BCa CI Lower	BCa CI Upper	Regression Coefficient	P-value	N CI Lower	N CI Upper	BCa CI Lower	BCa CI Upper
α-HCH	0.066	0.748	-0.337	0.469	-0.398	0.408	-0.058	0.849	-0.658	0.542	-0.587	0.550
HCB	-0.006	0.963	-0.251	0.239	-0.252	0.237	-0.100	0.628	-0.507	0.306	-0.523	0.288
mirex	0.165	0.259	-0.121	0.450	-0.130	0.444	-0.096	0.722	-0.624	0.433	-0.609	0.444
2,4′-DDE	0.782	0.050	0.001	1.563	0.059	1.493	-1.108	0.040	-2.166	-0.051	-2.339	-0.133
4,4′-DDE	0.138	0.298	-0.122	0.399	-0.140	0.378	-0.433	0.057	-0.878	0.013	-0.875	0.044
cis-chlordane	-1.205	<0.001	-1.858	-0.553	-1.693	-0.549	-0.144	0.794	-1.220	0.933	-1.244	0.971
cis-nonachlor	0.751	0.143	-0.253	1.756	-0.245	1.791	-1.213	0.177	-2.972	0.547	-3.057	0.467
heptachlor epoxide	0.602	0.005	0.179	1.026	0.163	1.005	-0.274	0.398	-0.907	0.360	-0.964	0.330
oxychlordane	0.752	<0.001	0.364	1.140	0.334	1.105	0.144	0.648	-0.473	0.760	-0.459	0.769
PCB-28+31	-0.480	0.006	-0.824	-0.135	-0.811	-0.120	-0.304	0.304	-0.882	0.275	-0.912	0.225
PCB-49	0.349	0.388	-0.445	1.144	-0.333	1.130	-2.248	0.002	-3.641	-0.856	-3.581	-0.850
PCB-52	0.742	0.036	0.050	1.435	0.123	1.397	-2.551	0.001	-4.002	-1.100	-3.920	-0.915
PCB-56	1.875	0.003	0.621	3.129	0.751	3.118	-2.385	0.032	-4.568	-0.203	-4.352	0.094
PCB-66	-0.339	0.041	-0.664	-0.013	-0.664	0.008	-0.346	0.304	-1.004	0.313	-1.144	0.222
PCB-70	1.100	0.008	0.288	1.912	0.248	1.905	-2.704	<0.001	-4.175	-1.233	-4.192	-1.215
PCB-74	1.443	0.011	0.330	2.556	0.565	2.380	-1.088	0.113	-2.435	0.259	-2.508	0.331
PCB-87	-0.378	0.453	-1.363	0.608	-1.456	0.472	0.466	0.323	-0.457	1.389	-0.533	1.314
PCB-92	1.075	<0.001	0.510	1.640	0.555	1.714	-1.562	0.001	-2.453	-0.671	-2.477	-0.700
PCB-99	-0.058	0.842	-0.629	0.513	-0.579	0.566	-0.660	0.235	-1.749	0.429	-1.826	0.316
PCB-101	1.570	0.011	0.364	2.776	0.182	2.669	-2.168	0.012	-3.858	-0.479	-3.797	-0.456
PCB-105	-0.204	0.201	-0.516	0.109	-0.579	0.061	-0.063	0.802	-0.554	0.428	-0.528	0.443
PCB-106	1.794	<0.001	1.264	2.324	1.285	2.310	-1.964	<0.001	-2.979	-0.949	-3.035	-1.023
PCB-114	0.069	0.775	-0.406	0.545	-0.358	0.468	0.239	0.505	-0.464	0.942	-0.394	1.012
PCB-118	-0.147	0.391	-0.482	0.189	-0.506	0.177	-0.265	0.366	-0.841	0.311	-0.924	0.220
PCB-119	-1.255	0.079	-2.653	0.144	-2.328	0.065	-0.102	0.931	-2.400	2.197	-2.034	2.414
PCB-128	-0.144	0.526	-0.590	0.302	-0.606	0.297	-0.326	0.408	-1.099	0.447	-1.139	0.383
PCB-130	-0.189	0.491	-0.728	0.349	-0.746	0.337	-0.411	0.321	-1.223	0.400	-1.307	0.334
PCB-137	-0.032	0.928	-0.722	0.658	-0.621	0.769	-1.054	0.093	-2.283	0.176	-2.258	0.188
PCB-138	0.148	0.608	-0.417	0.712	-0.365	0.785	-0.742	0.173	-1.811	0.326	-1.981	0.172
PCB-146	-0.107	0.541	-0.450	0.236	-0.454	0.252	-0.459	0.108	-1.018	0.100	-1.110	0.017
PCB-149	0.641	0.137	-0.203	1.486	-0.068	1.440	-1.280	0.028	-2.424	-0.136	-2.520	-0.167
PCB-153+132	0.030	0.914	-0.505	0.564	-0.446	0.708	-0.631	0.140	-1.469	0.207	-1.489	0.206
PCB-154	-0.353	0.273	-0.984	0.278	-0.968	0.205	-1.570	0.006	-2.689	-0.452	-2.818	-0.542
PCB-157	0.548	0.023	0.077	1.019	0.135	1.007	-1.023	0.003	-1.687	-0.359	-1.727	-0.327
PCB-158	0.483	0.108	-0.106	1.071	-0.042	1.150	-0.529	0.236	-1.405	0.346	-1.389	0.354
PCB-163	-0.135	0.456	-0.491	0.220	-0.494	0.194	-0.256	0.412	-0.870	0.357	-0.875	0.417
PCB-165	1.004	0.002	0.383	1.625	0.431	1.625	-1.645	0.001	-2.598	-0.692	-2.599	-0.762
PCB-166	0.441	0.042	0.016	0.865	0.048	0.882	-1.352	<0.001	-1.796	-0.909	-1.803	-0.915
PCB-167	0.327	0.180	-0.151	0.806	-0.121	0.845	-0.684	0.041	-1.342	-0.027	-1.353	-0.047
PCB-170	0.212	0.346	-0.229	0.653	-0.235	0.662	-0.451	0.212	-1.158	0.257	-1.159	0.322
PCB-172	0.116	0.600	-0.317	0.549	-0.256	0.583	-0.279	0.368	-0.885	0.328	-0.871	0.345
PCB-174	0.930	0.009	0.230	1.631	0.261	1.659	-1.743	<0.001	-2.692	-0.795	-2.740	-0.870
PCB-175	0.747	<0.001	0.333	1.162	0.357	1.178	-0.937	0.003	-1.554	-0.320	-1.493	-0.217
PCB-177	0.439	0.292	-0.377	1.255	-0.347	1.253	-0.682	0.315	-2.012	0.648	-2.170	0.540
PCB-178	0.756	0.016	0.143	1.368	0.127	1.381	-0.402	0.307	-1.175	0.370	-1.161	0.407
PCB-180+193	0.204	0.446	-0.321	0.729	-0.239	0.927	-0.694	0.086	-1.485	0.097	-1.476	0.103
PCB-183	0.080	0.676	-0.296	0.457	-0.301	0.467	-0.371	0.230	-0.977	0.235	-0.937	0.314
PCB-187	0.147	0.505	-0.285	0.579	-0.335	0.525	-0.365	0.312	-1.072	0.343	-1.120	0.322
PCB-188	1.471	<0.001	0.937	2.006	0.936	1.972	-2.048	<0.001	-2.726	-1.369	-2.691	-1.322
PCB-189	0.140	0.805	-0.975	1.255	-0.816	1.384	-0.091	0.821	-0.879	0.697	-0.904	0.694
PCB-191	0.101	0.814	-0.741	0.943	-0.408	0.945	-1.213	0.032	-2.319	-0.106	-2.299	-0.172
PCB-194	0.608	0.017	0.108	1.108	0.146	1.141	-0.007	0.987	-0.827	0.813	-0.862	0.800
PCB-195	-0.022	0.934	-0.543	0.499	-0.518	0.502	0.012	0.975	-0.766	0.791	-0.782	0.802
PCB-196	-0.052	0.835	-0.542	0.438	-0.502	0.514	-0.410	0.215	-1.058	0.238	-1.020	0.287
PCB-197	0.568	0.041	0.023	1.112	0.102	1.219	-1.040	0.001	-1.675	-0.406	-1.650	-0.354
PCB-199	-0.019	0.944	-0.550	0.512	-0.511	0.512	-0.271	0.421	-0.929	0.388	-0.937	0.417
PCB-201	0.680	0.002	0.245	1.115	0.256	1.107	-0.686	0.043	-1.351	-0.022	-1.335	-0.030
PCB-202	1.156	<0.001	0.519	1.794	0.596	1.902	-1.645	0.008	-2.860	-0.430	-2.684	-0.217
PCB-205	1.016	0.002	0.366	1.666	0.440	1.602	-1.321	0.001	-2.102	-0.539	-2.090	-0.564
PCB-206	0.342	0.276	-0.274	0.958	-0.201	0.966	-0.232	0.587	-1.067	0.604	-1.189	0.564
PCB-207	0.076	0.700	-0.312	0.464	-0.292	0.506	-0.195	0.511	-0.775	0.386	-0.765	0.360
PCB-208	0.301	0.361	-0.344	0.945	-0.230	1.077	-0.523	0.114	-1.171	0.126	-1.136	0.176
PBDE-47	0.134	0.768	-0.754	1.021	-0.776	0.904	-1.118	0.147	-2.629	0.394	-2.693	0.469
PBDE-99	-0.645	0.122	-1.464	0.174	-1.357	0.333	-2.140	<0.001	-3.200	-1.079	-3.257	-1.083
PBDE-100	-0.618	0.170	-1.500	0.265	-1.476	0.308	-1.064	0.129	-2.438	0.310	-2.535	0.316

Table 3. Comparison of bootstrapped normal (N) and bias-corrected and accelerated (BCa) 95% confidence intervals (CIs) of the coefficients from the piecewise log-linear spline regression models for each contaminant measured in thick-billed murre eggs.

	La Niña Phase						El Niño Phase					
Contaminant	Regression Coefficient	P-value	N CI Lower	N CI Upper	BCa CI Lower	BCa CI Upper	Regression Coefficient	P-value	N CI Lower	N CI Upper	BCa CI Lower	BCa CI Upper
α-HCH	0.197	0.703	-0.814	1.208	-0.649	1.436	1.501	<0.001	0.763	2.240	0.800	2.315
HCB	-0.087	0.799	-0.762	0.587	-0.740	0.647	0.008	0.978	-0.582	0.599	-0.594	0.606
2,4′-DDE	-2.085	0.031	-3.982	-0.189	-3.988	-0.279	-0.939	0.083	-2.000	0.122	-2.135	0.026
4,4′-DDE	-0.703	0.032	-1.346	-0.060	-1.348	-0.061	0.135	0.660	-0.468	0.739	-0.407	0.759
cis-nonachlor	-0.336	0.728	-2.229	1.557	-2.090	1.785	1.024	0.112	-0.239	2.288	-0.301	2.214
heptachlor epoxide	3.477	<0.001	1.523	5.431	1.363	5.335	-1.265	0.030	-2.411	-0.120	-2.467	-0.168
oxychlordane	-0.256	0.445	-0.912	0.400	-0.907	0.404	0.791	0.009	0.194	1.387	0.193	1.424
dieldrin	3.350	0.053	-0.046	6.747	0.385	7.366	1.908	0.113	-0.451	4.266	-0.269	4.379
PCB-28+31	-0.299	0.477	-1.123	0.525	-1.142	0.498	0.237	0.365	-0.276	0.750	-0.275	0.726
PCB-49	0.558	0.365	-0.649	1.766	-0.805	1.666	0.322	0.590	-0.849	1.492	-0.731	1.780
PCB-52	-1.741	0.098	-3.801	0.319	-3.712	0.371	1.581	0.012	0.342	2.820	0.441	2.905
PCB-56	-1.420	0.046	-2.813	-0.028	-2.944	-0.192	1.776	0.003	0.621	2.932	0.828	3.155
PCB-63	3.675	<0.001	2.447	4.903	2.340	4.903	-0.748	0.077	-1.576	0.080	-1.745	0.002
PCB-66	-1.017	0.004	-1.714	-0.321	-1.700	-0.277	0.559	0.083	-0.073	1.191	-0.085	1.165
PCB-70	-2.249	0.001	-3.574	-0.923	-3.553	-0.915	1.795	0.001	0.776	2.814	0.771	2.886
PCB-87	-0.132	0.878	-1.829	1.564	-1.898	1.492	1.668	<0.001	0.857	2.479	0.769	2.406
PCB-92	-0.806	0.664	-4.444	2.833	-4.430	3.291	-0.030	0.942	-0.855	0.794	-0.801	0.851
PCB-99	-1.968	0.001	-3.082	-0.853	-3.052	-0.852	1.710	0.002	0.654	2.766	0.705	2.741
PCB-101	-0.753	0.798	-6.522	5.017	-7.003	4.769	1.537	0.067	-0.106	3.180	-0.410	2.918
PCB-105	-1.093	<0.001	-1.671	-0.516	-1.654	-0.529	0.764	0.010	0.183	1.345	0.194	1.329
PCB-106	-1.442	0.639	-7.468	4.583	-6.121	6.233	0.206	0.598	-0.560	0.972	-0.506	1.021
PCB-114	-4.278	<0.001	-5.047	-3.510	-4.987	-3.406	1.436	<0.001	0.945	1.927	0.951	1.931
PCB-118	-1.639	0.057	-3.330	0.051	-3.483	-0.177	1.008	0.003	0.335	1.681	0.213	1.619
PCB-128	0.322	0.823	-2.507	3.151	-2.890	2.860	1.542	<0.001	0.750	2.334	0.770	2.351
PCB-130	-4.302	<0.001	-6.157	-2.447	-6.012	-2.222	1.115	0.012	0.244	1.986	-0.013	1.828
PCB-138	-1.876	0.001	-2.953	-0.798	-2.948	-0.752	1.795	0.001	0.697	2.893	0.702	2.900
PCB-146	-1.464	<0.001	-2.183	-0.745	-2.206	-0.692	1.128	0.002	0.425	1.831	0.435	1.824
PCB-149	1.861	0.001	0.788	2.933	0.747	2.926	-0.269	0.590	-1.244	0.707	-1.305	0.688
PCB-153+132	-6.290	0.145	-14.744	2.163	-16.626	1.147	1.627	0.001	0.653	2.602	0.638	2.540
PCB-154	-1.682	0.094	-3.654	0.289	-3.287	0.779	0.899	0.120	-0.233	2.032	-0.456	1.811
PCB-156+202+171	-0.874	0.060	-1.787	0.039	-1.767	0.079	0.280	0.486	-0.508	1.069	-0.718	0.953
PCB-157	1.469	0.020	0.236	2.702	0.377	2.901	-1.081	0.049	-2.157	-0.004	-2.433	-0.177
PCB-158	-2.644	<0.001	-3.851	-1.438	-4.167	-1.621	2.987	<0.001	1.892	4.081	2.108	4.437
PCB-163	-1.422	<0.001	-2.150	-0.693	-2.171	-0.726	1.277	0.001	0.549	2.005	0.585	2.021
PCB-165	-1.189	0.104	-2.622	0.243	-2.692	0.153	0.533	0.236	-0.349	1.414	-0.359	1.429
PCB-166	-1.589	0.002	-2.590	-0.588	-2.321	-0.195	0.187	0.441	-0.288	0.662	-0.427	0.599
PCB-170	-0.586	0.173	-1.428	0.256	-1.435	0.267	1.072	0.012	0.234	1.909	0.204	1.891
PCB-172	-1.344	0.009	-2.353	-0.335	-2.240	-0.229	0.985	0.002	0.358	1.612	0.324	1.602
PCB-175	-1.398	0.024	-2.615	-0.181	-2.484	-0.071	0.796	0.048	0.005	1.586	-0.064	1.577
PCB-177	-1.511	0.127	-3.451	0.428	-3.344	0.471	1.625	0.003	0.569	2.680	0.433	2.616
PCB-178	-0.179	0.781	-1.437	1.080	-1.365	1.171	0.768	0.041	0.033	1.502	-0.064	1.441
PCB-180+193	-1.441	0.071	-3.006	0.123	-2.881	0.220	1.850	<0.001	0.835	2.866	0.759	2.750
PCB-183	-1.500	<0.001	-2.246	-0.755	-2.348	-0.811	1.569	<0.001	0.836	2.303	0.902	2.329
PCB-187	-1.336	<0.001	-2.072	-0.600	-2.106	-0.684	1.545	<0.001	0.804	2.286	0.894	2.391
PCB-188	-0.626	0.438	-2.206	0.955	-2.952	0.529	-0.434	0.417	-1.482	0.615	-1.157	1.275
PCB-189	-1.910	0.003	-3.169	-0.652	-3.047	-0.510	1.179	0.002	0.449	1.910	0.482	1.946
PCB-191	-1.671	0.099	-3.658	0.316	-3.512	0.450	1.188	0.040	0.054	2.321	0.004	2.248
PCB-194	1.841	0.001	0.764	2.917	0.861	2.979	-0.258	0.609	-1.248	0.732	-1.379	0.615
PCB-195	1.076	0.026	0.127	2.024	0.105	2.088	0.802	0.079	-0.093	1.696	-0.093	1.659
PCB-196	0.306	0.896	-4.287	4.900	-3.491	5.807	1.336	0.006	0.383	2.289	0.447	2.381
PCB-197	-0.763	0.323	-2.275	0.749	-2.227	0.809	0.873	0.060	-0.037	1.783	-0.143	1.811
PCB-199	-0.531	0.414	-1.807	0.744	-1.782	0.740	1.037	0.004	0.322	1.752	0.388	1.801
PCB-201	-5.041	<0.001	-6.276	-3.807	-6.552	-4.056	2.800	<0.001	1.629	3.971	1.898	4.310
PCB-202	9.233	0.011	2.137	16.329	2.905	17.744	-0.364	0.618	-1.796	1.067	-1.834	1.067
PCB-205	-3.939	0.228	-10.337	2.459	-10.744	2.059	-0.219	0.689	-1.290	0.852	-1.575	0.716
PCB-206	1.623	0.005	0.497	2.748	0.540	2.736	-0.014	0.979	-1.073	1.045	-1.058	1.098
PCB-207	-1.539	0.009	-2.697	-0.381	-2.597	-0.318	0.995	0.006	0.290	1.701	0.275	1.674
PCB-208	-2.130	0.003	-3.547	-0.713	-3.570	-0.751	0.855	0.034	0.065	1.645	0.127	1.666
PCB-209	3.185	<0.001	2.201	4.168	2.063	4.042	0.078	0.870	-0.858	1.015	-0.851	1.038
PBDE-47	-0.797	0.457	-2.896	1.302	-2.704	1.590	2.814	<0.001	1.412	4.216	1.165	4.058
PBDE-99	0.061	0.959	-2.267	2.388	-2.450	2.311	0.676	0.368	-0.795	2.148	-0.790	2.224
PBDE-100	-2.129	0.089	-4.582	0.324	-4.402	0.206	2.142	0.005	0.652	3.632	0.449	3.527

Table 4. Relative contribution of each PCB congener to the total PCB concentration and their measurement frequencies.

Homolog	PCB Congener	Contribution (%)	Measurement frequency (%)
Trichlorobiphenyl	PCB-28+31	3.13	86.9
Tetrachlorobiphenyl	PCB-49	0.09	100
	PCB-52	0.23	100
	PCB-56	1.33	100
	PCB-63	0.38	100
	PCB-066	3.44	100
	PCB-70	0.15	100
	PCB-74	2.44	100
Pentachlorobiphenyl	PCB-87	0.19	91.1
	PCB-92	0.13	91.1
	PCB-99	6.57	100
	PCB-101	0.45	91.1
	PCB-105	3.22	100
	PCB-106	0.08	77.9
	PCB-107	0.74	100
	PCB-114	0.31	86.9
	PCB-118	10.10	91.1
	PCB-119	0.12	86.9
Hexachlorobiphenyl	PCB-128	1.38	91.1
	PCB-130	0.58	86.9
	PCB-137	0.36	86.9
	PCB-138	8.60	100
	PCB-146	4.33	100
	PCB-149	0.52	100
	PCB-153+132	19.37	77.9
	PCB-154	0.10	86.9
	PCB-157	0.26	100
	PCB-158	0.49	100
	PCB-163	4.22	100
	PCB-165	0.06	86.9
	PCB-166	0.11	86.9
	PCB-167	0.67	86.9
Heptachlorobiphenyl	PCB-170	2.45	100
	PCB-172	0.83	86.9
	PCB-174	0.09	100
	PCB-175	0.18	86.9
	PCB-177	0.68	86.9
	PCB-178	0.78	86.9
	PCB-180+193	5.24	86.9
	PCB-183	1.67	100
	PCB-187	6.52	100
	PCB-188	0.06	86.9
	PCB-189	0.14	86.9
	PCB-191	0.04	86.9
Octachlorobiphenyl	PCB-194	1.10	100
	PCB-195	0.40	100
	PCB-196	1.41	77.9
	PCB-197	0.11	86.9
	PCB-199	1.78	86.9
	PCB-201	0.30	100
	PCB-202	0.09	77.9
	PCB-205	0.07	77.9
Nonachlorobiphenyl	PCB-206	0.44	100
	PCB-207	0.11	86.9
	PCB-208	0.19	86.9
Decachlorobiphenyl	PCB-209	0.32	100
Mixed	PCB-156+202+171	0.94	100

Figure 1. Association between ONI index and contaminant levels measured in thick-billed murre (*Uria lomvia*) eggs, grouped by contaminant type (PCB, OCP, and PBDE). Points represent the regression coefficient for each lipid-adjusted and natural log-transformed contaminant during the El Niño (red) and La Niña (blue) phases of the ENSO, after adjusting for PDO index, year, and waterbody. Pooled estimates from the meta-analysis (denoted as plus symbols) are included. Lines represent the corresponding 95% normal bootstrapped confidence intervals.

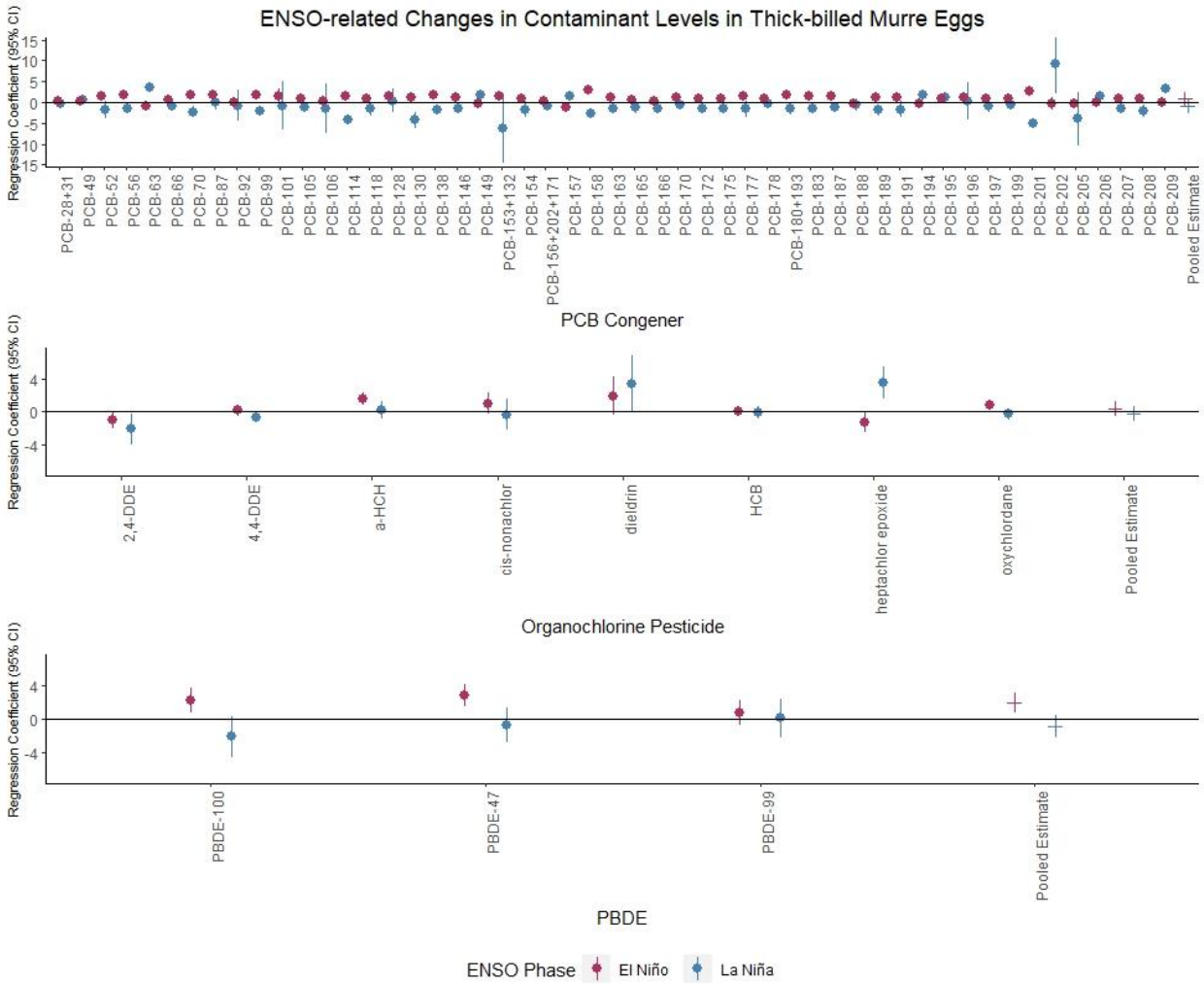

Figure 2. Association between ONI index and contaminant levels measured in common murre (*Uria aalge*) eggs, grouped by contaminant type (PCB, OCP, or PBDE). Points represent the regression coefficient for each lipid-adjusted and natural log-transformed contaminant during the El Niño (red) and La Niña (blue) phases of the ENSO, after adjusting for PDO index, year, and waterbody. Pooled estimates from the meta-analysis (denoted as plus symbols) are included. Lines represent the 95% bootstrapped normal confidence intervals.

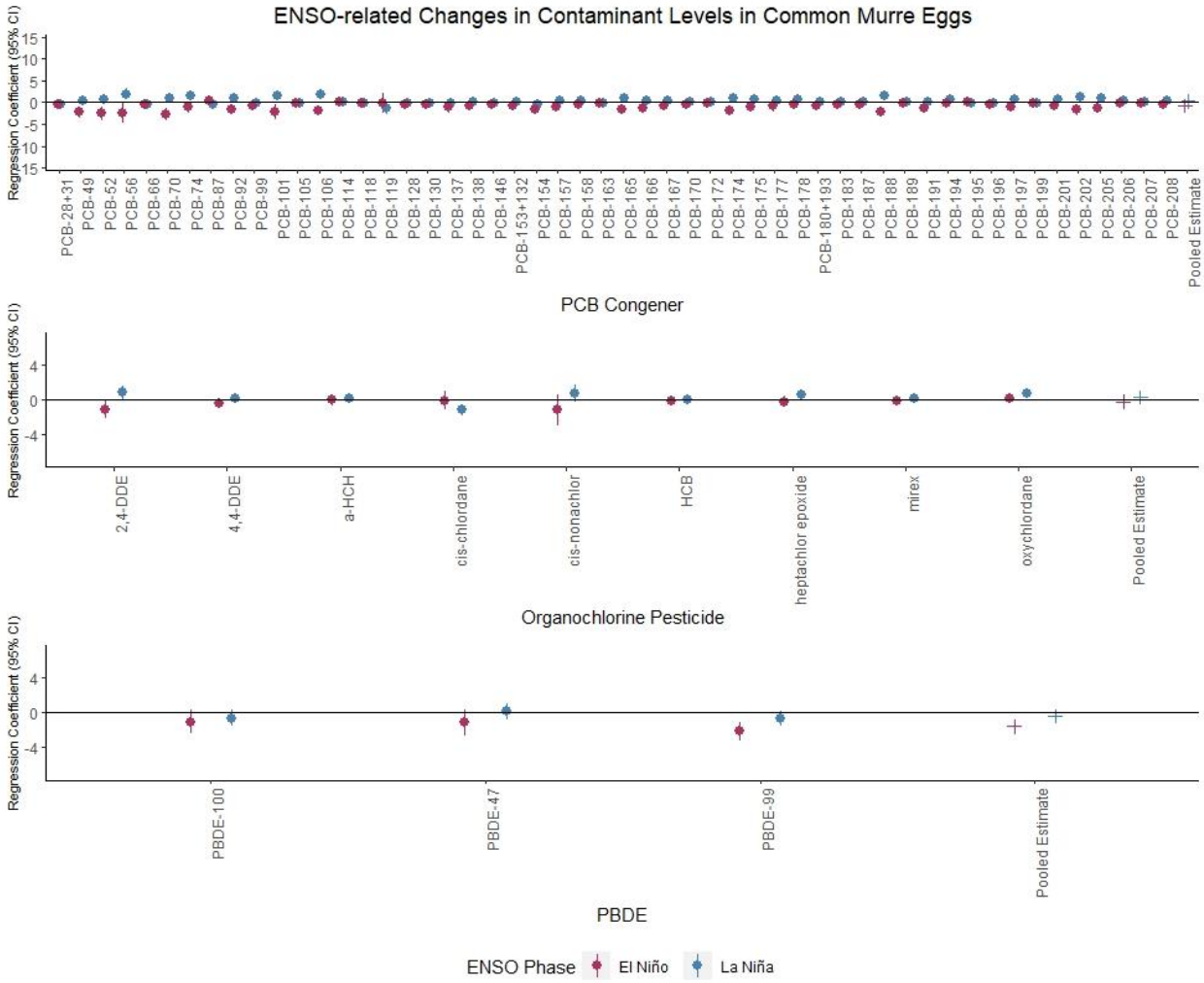

Figure 3. PCB congener levels measured in thick-billed murre eggs conditioned on relative abundance of each congener within the sample. Each circle represents the regression coefficient from the fully adjusted, piecewise log-linear spline models for each congener, stratified by ENSO phase. Circle sizes are proportional to the precision of each regression coefficient. 95% confidence intervals are shown as grey bands.

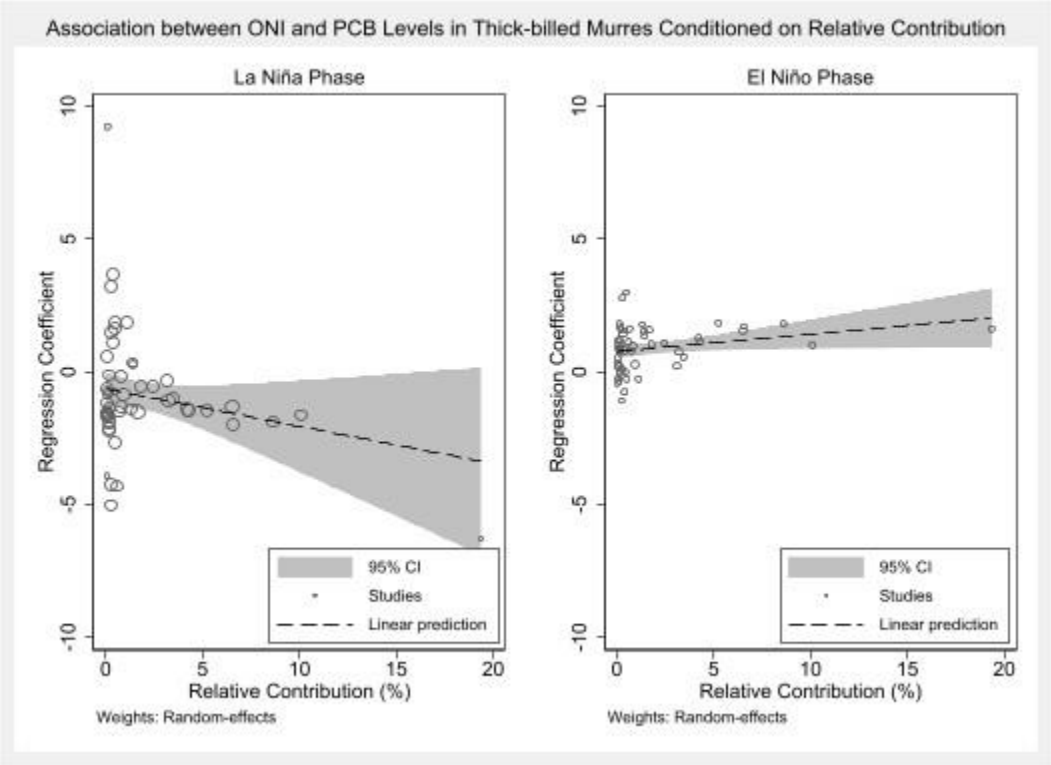

Figure 4. PCB congener levels measured in common murre eggs conditioned on relative abundance of each congener within the sample. Each circle represents the regression coefficient from the fully adjusted, piecewise log-linear spline models for each congener, stratified by ENSO phase. Circle sizes are proportional to the precision of each regression coefficient. 95% confidence intervals are shown as grey bands.